

Electronic structure and magnetocrystalline anisotropy in Fe–Co–Ni binary alloy monolayers on Cu(001)

Horng-Tay Jeng^{a,b,*}, Ding-Sheng Wang^c

^a*Institute of Physics, Academia Sinica, Taipei 11529, Taiwan*

^b*Department of Physics, National Tsing Hua University, Hsinchu 300, Taiwan*

^c*Institute of Physics, Chinese Academy of Sciences, Beijing 100080, China*

Received 12 February 2007; received in revised form 23 April 2007

Available online 8 May 2007

Abstract

The electronic structures and magnetocrystalline anisotropy (MCA) energies of Fe–Co–Ni binary alloy monolayers on Cu(001) substrate under structural optimization have been investigated using the generalized gradient approximation. Isolated Fe–Co–Ni alloy monolayers are also studied for comparison. It is found that there exists a Slater–Pauling curve for the averaged magnetic moment of these alloying monolayers, whereas no such curve was found for the MCA energies. In addition to the perpendicular magnetization obtained for pure Fe and in-plane magnetization obtained for pure Co and Ni monolayers, a spin-reorientation transition upon a variation of the Fe concentration is observed in Fe–Co and Fe–Ni systems.

© 2007 Elsevier B.V. All rights reserved.

PACS: 75.30.Gw; 75.30.Pd; 75.70.Ak

Keywords: Magnetocrystalline anisotropy; Alloy monolayer; Spin-reorientation transition

1. Introduction

Magnetocrystalline anisotropy (MCA), originally proposed by van Vleck [1] to be a consequence of spin–orbit coupling more than 60 years ago, remains to be one of the most interesting and challenging research areas of ferromagnetic materials both experimentally and theoretically. Because of the continuous improvement in growing magnetic thin films as well as in theoretical treatment on magnetic anisotropy of multilayers, the effects of reduced dimensionality on magnetic properties of thin films have attracted much more attention in recent years. Experiments have revealed that many overlayer and superlattice systems show perpendicular magnetizations. Moreover, there exists spin-reorientation transitions from perpendicular to in-plane magnetization or vice versa [2–7] with respect to certain conditions such as composed species, layer thick-

ness, temperature, alloy concentration, and even the supporting substrates. These phenomena are not only of great scientific interests but also fairly potential for industrial applications such as high-density magneto-optical storage media. It is therefore interesting to investigate the fundamental physics of the magnetic anisotropy and the underlying mechanism of the magnetization reorientation in thin films.

The pioneering theoretical work on the MCA of free-standing monolayers at the Ag lattice constant was done by Gay and Richter [8,9]. They found that the easy direction of magnetization is perpendicular to the plane of the monolayer for Fe and V, but in the plane for Ni and Co. Determination of the strain effect on the MCA energy of a free-standing Fe monolayer with lattice constant of Cu, Ag, and W [10] shows that along with increasing lattice parameter, the magnetic moment is enhanced, whereas the anisotropy constant decreases with the out-of-plane anisotropy remaining unchanged. Similar trend that the sign of MCA energy is insensitive to the lattice strain has also been found in the in-plane magnetization of Co

*Corresponding author. Institute of Physics, Academia Sinica, Taipei 11529, Taiwan. Tel.: +886 2 27896765; fax: +886 2 27834187.

E-mail address: jeng@phys.sinica.edu.tw (H.-T. Jeng).

monolayer [11,12]. Recent works on the MCA energy have been extended to systems of lower dimensionality such as step edges [13] and monoatomic wires [14].

Although there have been many theoretical works investigating the MCA energy of Fe-, Co-, and Ni-related overlayer, interlayer, multilayer, and so on [11,15–19], to our knowledge, there is no published result for an Fe–Co–Ni alloying monolayer of certain composition on a nonmagnetic supporting substrate. Since the switching behavior of the spin-reorientation transition could be manipulated by varying the alloy compositions experimentally, therefore this phenomenon could be of great industrial importance, and a theoretical investigation on the underlying physics is necessary. In this work, we investigate the effects of different alloy compositions on electronic and magnetic properties as well as on the MCA energies of the Fe–Co–Ni alloy monolayers on Cu(001) substrate under structural optimization using the VASP package [20]. The pure Fe, Co, and Ni monolayers on Cu(001) and also the isolated alloy monolayers are studied for comparison. The computational details are summarized in the following section. The calculated results are presented and discussed in detail in Section 3. The conclusions are given in Section 4.

2. Computational details

The self-consistent electronic structure calculations were performed using the highly accurate frozen-core full-potential projector augmented wave method [21], as implemented in the VASP package [20], based on the generalized gradient approximation (GGA) [22]. Both the Fe–Co–Ni alloy monolayers on Cu(001) substrate under structure optimization and the isolate Fe–Co–Ni alloy monolayers are calculated for comparison. For the latter case, we approximate a monolayer supported on a nonmagnetic substrate using a free-standing monolayer with lattice constant matching the ideal FCC Cu(001) surface. For the former case, we used a three-layer Cu(001) slab to model the substrate with both sides of the Cu slab covered by Fe–Co–Ni alloy monolayers at the FCC-site. We firstly optimize the lattice structure on 78 k -points over the irreducible two-dimensional Brillouin zone. Then we calculate the MCA energy ($E[100] - E[001]$, where E is the total energy) by incorporating the spin–orbit coupling in the self-consistent calculations on 300 k -points over the irreducible two-dimensional Brillouin zone with the magnetization orientation along perpendicular ([001]) and in-plane ([100]) directions separately. To ensure the calculations be sufficiently accurate, 46060 plane waves with the cut-off energy of 273 eV were used in the calculations.

3. Results and discussions

The general trend of the lattice optimization reveal that the interlayer spacing between the overlayer (Fe–Co–Ni

binary alloying monolayer) and the first subsurface layer (outermost Cu layer) is smaller than the bulk value, while the interlayer distance between the first and second subsurface layers is larger than the bulk value. This is in agreement with the general trend of surface relaxation [23]. To illustrate the evolution of density of states (DOS) from high concentration towards low concentration in Fe–Ni alloy monolayers, we present in Fig. 1 the DOS of Fe (left panels, (a)–(d)) and Ni (right panels, (e)–(h)) in Fe–Ni monolayer on Cu(001) substrate with 100%, 75%, 50%, 25%, and 0% Fe concentrations, respectively, under lattice relaxation. Along with decreasing Fe concentrations, the bandwidth of Fe-3d is narrowed down because of increasing Ni neighbors, whereas the Ni bandwidth is enhanced and the band energy is raised, especially in the spin down channel. Meanwhile, the exchange splitting of Fe is enhanced and the spin down states are less occupied, indicating an increment of magnetic moment of Fe. Whereas Ni-3d is affected in the opposite way that the spin down unoccupied states are decreased, giving rise to suppressed magnetic moments. The above phenomena reveal that the charge transfer from low- Z Fe to high- Z Ni atoms plays an important role in the magnetic behavior of alloying monolayers. Note that DOS of Fe never approaches that of Ni at any low Fe concentrations considered in this work ((d) and (h)), and the influence of Ni on DOS of Fe saturates as the Fe concentration is lower than 25% since all the first and second nearest neighbors of Fe are already Ni. As a result, the charge- and spin-density distributions are closer to the localized electron picture in an alloying monolayer system. Further, the neutrality condition is more or less reserved, and each component maintains to some extent its own character, indicating that the simple rigid-band filling model or the convenient virtual crystal approximation may not be adequate for describing such alloying system. Similar trends have also been found in Fe–Co and Co–Ni alloying monolayers which are not shown here.

Table 1 lists calculated charge in 3d orbitals, total valence charge, magnetic moment, and also MCA energy of pure Fe, Co, and Ni in bulk states, free-standing monolayers, and monolayers on Cu(001) substrates under lattice relaxation. In comparison with the bulk systems, the relative charge transfers in the free-standing monolayer systems are from the 3d \downarrow to the 3d \uparrow orbitals as well as to the interstitial and vacuum regions, therefore leading to reduced valence charges and enhanced magnetic moments. The spin up 3d states are nearly filled with the number of electrons about the same, whereas in the spin down 3d orbitals, the occupancies are different from each other by about one electron, resulting in total magnetic moments of 2.97, 2.07, and $0.98\mu_B$ /atom for Fe, Co, and Ni, respectively. They are significantly larger than the bulk values (Table 1), and are consistent with published results [8–10,24]. In the Cu supported cases, the valence charges are increased because of the reduced vacuum regions, while the magnetic moments are suppressed to 2.78, 1.83, and

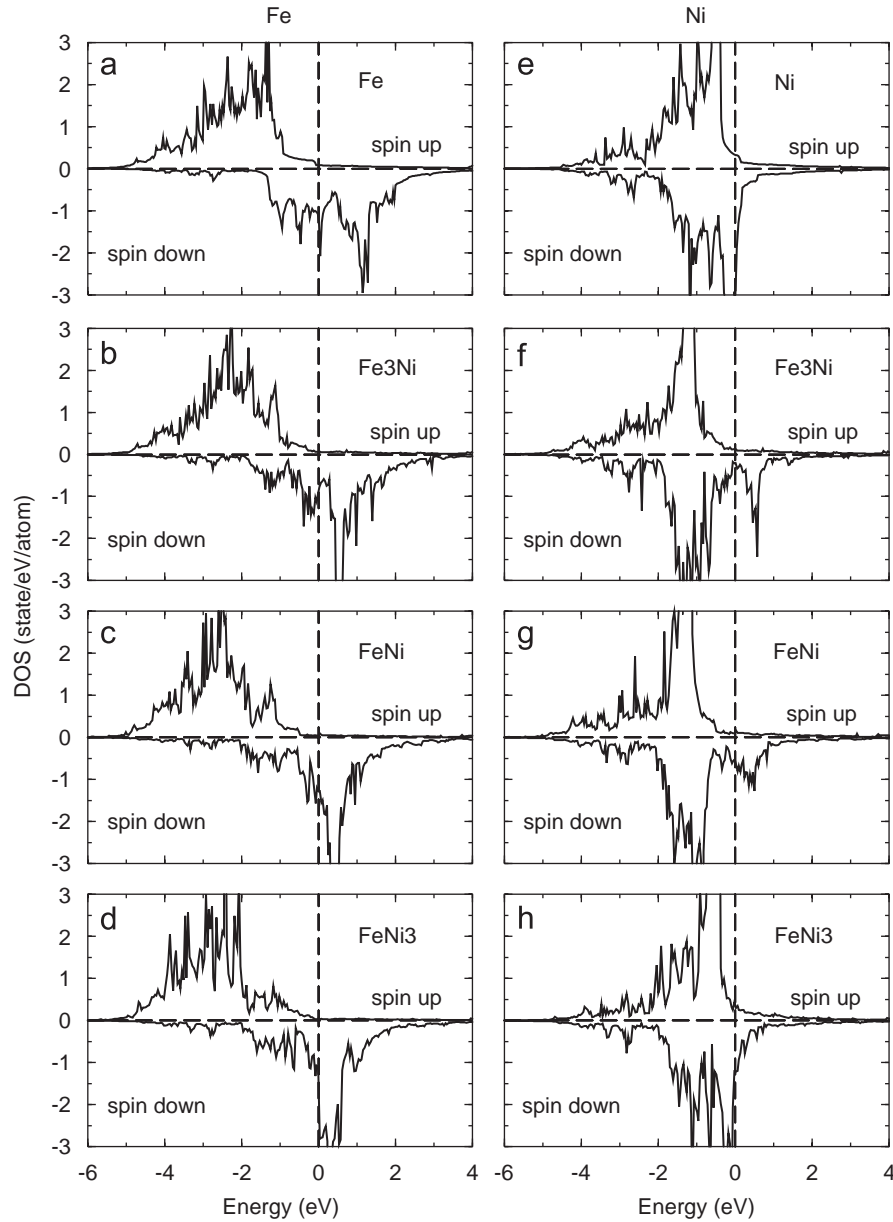


Fig. 1. Spin decomposed DOS of Fe-3d (left panels) and Ni-3d (right-panels) in Fe–Ni alloying monolayer over Cu(001) substrate under lattice optimization with Fe concentrations of 100% (a), 75% (b, f), 50% (c, g), 25% (d, h), and 0% (e). The Fermi level is at zero energy.

$0.44\mu_B/\text{atom}$, respectively, due to the nonmagnetic Cu atoms. The reduced magnetic moments of Fe/Cu and Co/Cu are still 0.51 and $0.19\mu_B/\text{atom}$ larger than the corresponding bulk values, respectively. Nevertheless, the resultant moment of Ni/Cu is $0.19\mu_B/\text{atom}$ less than that of bulk Ni. The opposite trend in Ni is closely related to the competition between the charge transfer directions and the exchange splitting suppressions induced by Cu substrates.

On the other hand, the calculated MCA energies ($E[100] - E[001]$) of pure Fe, Co, and Ni free-standing monolayers are, respectively, 0.63 , -1.26 , and -1.43 meV/atom (Table 1). The supporting nonmagnetic Cu(001) substrate to some extent suppresses the magnitude of MCA energies to 0.29 , -0.23 , and -1.24 meV/atom (Table 1) with the signs of

the MCA energies remaining unchanged. Consequently the Fe monolayer exhibits the perpendicular magnetization, whereas Ni and Co monolayers prefer the in-plane magnetization. Dittschar et al. [3] have measured the spin-orbit coupling caused anisotropy energy E_{soc} as a function of film thickness from two to four monolayers [3, Fig. 3]. If one extrapolates the line fitted to E_{soc} [3, Fig. 3] to monolayer thickness, the E_{soc} is 0.63 mJ/m², which corresponds to 0.26 meV/atom as listed in Table 1. This extrapolated E_{soc} in fact compares very well with our MCA energy of 0.29 meV/atom for pure Fe monolayer on Cu(001). Further, as listed in Table 1, all the calculated MCA energies and directions of easy axes using the VASP package are consistent with previous experimental [2–5] and theoretical [8–11,25] results.

Table 1

3d Charge (e), total valence charge (e), magnetic moment (μ_B), and MCA energy (meV/atom) of Fe, Co, and Ni bulk systems, free-standing monolayers (ML), and monolayers at FCC site upon three layers of Cu(001) substrates under structure relaxation (ML/Cu) using the VASP package. The charge and moment are integrated within atomic radius of 1.22 Å (2.31 Bohr radius). The Pauli electron negativity with +2 ionicity and other theoretical MCA energies are listed for comparison

	3d \uparrow charge	3d \downarrow charge	Valence charge	Magnetic moment	MCA energy	MCA energy	Electron negativity ^a
Fe (BCC)	4.14	1.83	6.59	2.27	–	–	1.83
Co (HCP)	4.37	2.69	7.74	1.64	–	–	1.88
Ni (FCC)	4.39	3.74	8.83	0.63	–	–	1.91
Fe (ML)	4.44	1.49	6.36	2.97	0.63	0.42 ^b	–
Co (ML)	4.53	2.47	7.44	2.07	–1.26	–1.35 ^c	–
Ni (ML)	4.55	3.57	8.56	0.98	–1.43	–	–
Fe (ML/Cu)	4.36	1.60	6.44	2.78	0.29	0.26 ^d	–
Co (ML/Cu)	4.44	2.61	7.56	1.83	–0.23	–	–
Ni (ML/Cu)	4.31	3.87	8.70	0.44	–1.24	–0.69 ^e	–

^aRef. [26].

^bRef. [10].

^cRef. [11].

^dRef. [3].

^eRef. [25].

Fig. 2 demonstrates the valence charge (a) and magnetic moment (b) with respect to the effective atomic number (Z) in Fe–Co–Ni alloy monolayers. We have shifted the results of pure Fe, Co, and Ni monolayers (Table 1) to zero in order that the charge and moment transfer among different species could be seen clearly. Take free-standing Fe–Ni system for example, the valence charge (Fig. 2(a)) of Fe is suppressed due to the increasing Ni neighbors, whereas that of Ni grows with increasing Fe neighbors, indicating the charge transfer from Fe of fewer valence electrons to Ni of more valence electrons. Although the direction of charge transfer is in some sense opposite to initial guess, this is, however, consistent with experimental experiences that Fe (Co) is easier to lose electrons than Co (Ni) due to the increasing Pauli electron negativity for larger Z species [26] as listed in Table 1. This is because of the stronger Coulomb attraction of a heavier nucleus and therefore the stronger binding and the smaller size of 3d orbitals. It can also be seen in the figure that the Cu substrate to some extent suppresses the charge transfer with the transfer directions remaining unchanged.

On the other hand, as shown in Fig. 2(b), magnetic moment of Fe in the free-standing Fe–Ni monolayer increases significantly with increasing Z , while moment of Ni decreases with decreasing Z , revealing the magnetic moment transfer from Ni to Fe. The opposite directions of transfer between charge and moment result from the fact that the charge transfer from Fe to Ni is dominated by the process from Fe-3d \downarrow orbital to Ni-3d \downarrow orbital. Meanwhile in the Cu supported Fe–Ni monolayers, the magnetic moment transfers in Fe are about the same as those in the free-standing cases, whereas the magnetic moment of Ni decreases with increasing Z . This opposite trend results from the competing suppressed exchange splitting induced by the nonmagnetic Cu substrates against the charge

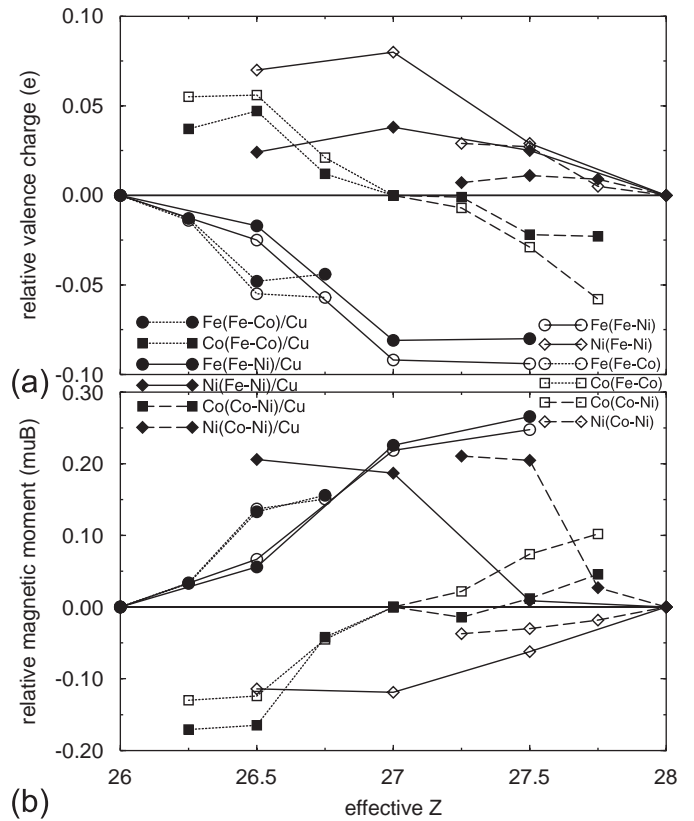


Fig. 2. Relative valence charge (a) and magnetic moment (b) in free-standing Fe–Co–Ni binary alloy monolayers (empty symbols) and in monolayers over Cu(001) substrate (solid symbols) under lattice relaxation. Results of pure Fe, Co, and Ni monolayers have been shifted to zero. The lines are a guide to the eye only.

transfer process from Fe-3d \downarrow to Ni-3d \downarrow orbital observed in the free-standing cases. Similar trend can also be found in Co–Ni monolayers. Note that the above mentioned

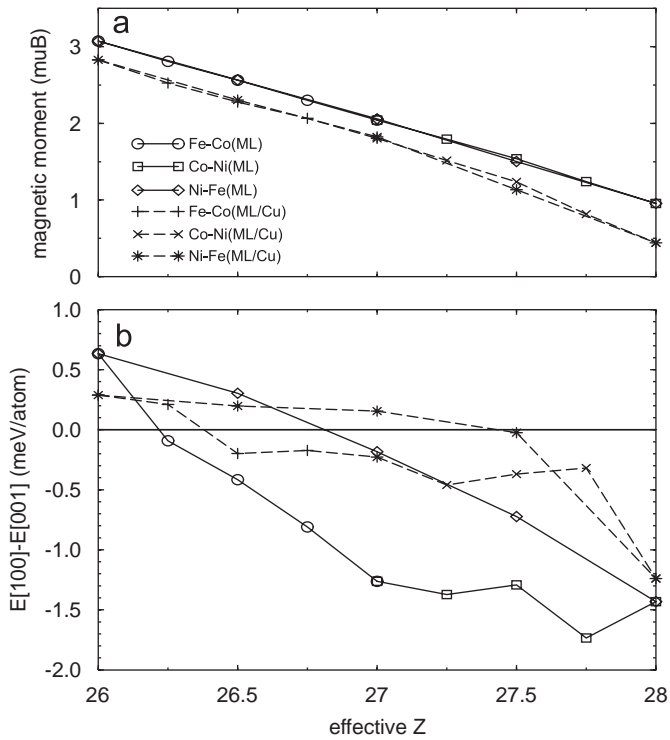


Fig. 3. Averaged magnetic moment (a) and MCA energy (b) in free-standing Fe–Co–Ni binary alloy monolayers (ML) and in corresponding monolayers over Cu(001) substrate (ML/Cu) under structure optimization. The lines are a guide to the eye only.

phenomenon is not found in the Fe–Co monolayers because of the relatively strong exchange splittings in Fe and Co atoms. The above discussions reveal in general that in Fe–Co–Ni alloy monolayers, charge transfers from low Z to high Z species, whereas the magnetic moment transfers are much more complicated, especially when the nonmagnetic Cu substrates are involved. Nevertheless, the magnitude of charge and moment transfers in all the considered cases are limited respectively within $0.10e$ and $0.30\mu_B$ (Fig. 2), indicating that the neutrality condition is approximately preserved.

It is well known that there exists in 3d alloy bulk systems both experimentally and theoretically a Slater–Pauling curve that in spite of different compositions of the system, the averaged magnetic moment depends linearly on the effective atomic number (Z) only. In Fig. 3(a), we present the averaged magnetic moment of Fe–Co–Ni alloy monolayer systems with or without Cu(001) substrate with respect to effective Z . Although the charge and magnetic moment transfers between different species (Fig. 2) are somewhat complicated, remarkably, the averaged magnetic moments of monolayer systems with different constituents well agree with each other, and simply fall in almost the same straight line. It can be seen in Fig. 3(a) that a Slater–Pauling curve for the averaged magnetic moment exists also in Fe–Co–Ni alloy monolayer systems no matter the Cu substrates exist or not. The nonmagnetic Cu(001) substrate affects the Slater–Pauling curve only quantita-

tively by a $0.2\text{--}0.5\mu_B$ reduction per atom in the averaged magnetic moment. This nonmagnetic substrate induced magnetic moment reduction is consistent with previous works [27]. The major difference between the Slater–Pauling curve of bulk crystal moment and the monolayer moment is that the bulk Fe–Co alloy show a moment maximum at about Co(30%)–Fe(70%), whereas this moment maximum does not exist in the Fe–Co alloy monolayers in both the free-standing and the Cu supported cases. From the results of this work, one could now predict the magnetic moment of a given monolayer, or design a monolayer with given magnetic moment. Note that such linear dependence could be explained fortuitously by the rigid-band filling model, since magnetic moments of individual atoms are similar to the pure monolayer cases and are therefore averaged linearly. However, as shown previously, the alloying systems are indeed closer to the localized electron picture, and the bandwidth and dispersion have been perturbed significantly. As a result, the simple rigid-band filling model would not be adequate for explaining the MCA energies as discussed below.

In Fig. 3(b), we summarize the calculated MCA energies of free-standing Fe–Co–Ni alloy monolayers as well as the corresponding monolayers on Cu(001) substrate with respect to effective Z . Interestingly, in both cases, the dependence of the MCA energy of Fe–Co, Co–Ni, and Fe–Ni on Z deviates from each other significantly. There exists no Slater–Pauling-like curve in the MCA energy as that in averaged magnetic moment (Fig. 3(a)). Take free-standing Fe–Ni alloying systems for example (Fig. 3(b)), the positive MCA energies (out-of-plane anisotropy) at high Fe concentrations decrease to negative values (in-plane anisotropy) at $Z \cong 26.8$. Whereas in free-standing Fe–Co systems, the MCA energies also vary from positive to negative with respect to increasing Z at a much higher rate. The perpendicular magnetization exists only at a low Co concentration ($<25\%$). As a result, the free-standing Fe–Co and Fe–Ni monolayers exhibit spin-reorientation transitions from in-plane to the plane normal with respect to decreasing Z at Fe concentrations of $\sim 75\%$ and $\sim 60\%$, respectively. On the other hand, the nonmagnetic Cu substrate suppresses the magnitude of MCA energy of the alloying monolayers significantly. Moreover, the Cu substrate also brings the MCA energy toward more positive (out-of-plane) as shown in the figure. Consequently the spin-reorientation transitions in Fe–Co/Cu and Fe–Ni/Cu systems from in-plane to the plane normal with respect to decreasing Z take place at lower Fe concentrations of $\sim 60\%$ and $\sim 25\%$, respectively. This effect has also been found in the Co–Cu interface and has been demonstrated to be a consequence of the strong interaction between the out-of-plane Co bonding z^2 , xz , and yz states and the Cu states, and therefore the suppressed negative contribution of the MCA energies [28]. Since Fe tends to reorient the in-plane anisotropy of Co and Ni into the out-of-plane anisotropy, one could thus manipulate the perpendicular and in-plane magnetizations experimentally by varying the

Fe concentrations in Fe–Co and Fe–Ni alloying monolayers. As for the Co–Ni monolayers, no such transition could be found because of the in-plane anisotropy of both the pure Co and Ni monolayers.

Fig. 3(b) also unravels that the simple rigid-band filling model is inadequate for describing the much more sophisticated MCA energies in all the considered cases. Within the rigid-band filling model, an Fe–Ni system at a certain Ni concentration is expected to have the same MCA energy as an Fe–Co system at a Co concentration twice larger than that of Ni in the Fe–Ni system. Thus the MCA energy of Fe–Ni system would fall along that line of Fe–Co system with twice higher the changing rate with respect to Z . Nevertheless, this is not the case as shown in Fig. 3(b). For example at $Z = 27$, the MCA energy of pure free-standing Co monolayer is far below that of Fe(50%)–Ni(50%) monolayer. Meanwhile in the case with Cu substrate, the MCA energies of pure Co and Fe(50%)–Ni(50%) monolayers are different even in sign because of the more-positive MCA energies induced by the Cu substrate. The former prefers the in-plane magnetization while the latter favors the perpendicular magnetization. This is because the MCA energy is closely related not only to the electron filling but also to the band dispersion, charge and moment transfer, as well as to the orbital character of the highest occupied states and the lowest empty states of Fe–Co–Ni alloy monolayers.

Another significant issue is whether or not the in-plane shape anisotropy would damage the obtained out-of-plane anisotropy. To clarify this issue, we calculated the shape anisotropy according to $2\pi M^2$, where M is the magnetization density, with our calculated mean magnetic density. Since the averaged magnetic moment decreases monotonically from $2.83\mu_B/\text{Fe}$ to $1.80\mu_B/\text{Co}$, the magnitude of the shape anisotropy also decreases monotonically from $0.23\text{ meV}/\text{Fe}$ to $0.09\text{ meV}/\text{Co}$. The obtained in-plane shape anisotropy energies are smaller than the calculated out-of-plane anisotropy energies of 0.29 and $0.15\text{ meV}/\text{atom}$ of the pure Fe monolayer and Fe(50%)–Ni(50%) alloy monolayer, respectively. As a result, the calculated out-of-plane anisotropy of the high Fe concentration alloy monolayers remain unchanged. On the other hand, if only the surface term exists, it would become in-plane magnetization when the pure Fe film is thicker than $0.29/0.23 = 1.3$ monolayer. However, as shown in Ref. [3, Fig. 3], the E_{soc} term has a bulk contribution and also increases with the thickness of the Fe films on Cu(001), keeping the out-of-plane anisotropy of thicker films.

4. Conclusions

We have systematically investigated the electronic structures and the MCA energies of free-standing as well as Cu(001) slab supported Fe–Co–Ni binary alloy monolayers. The DOS of each constitution is affected significantly by the other component in alloying systems. The charge transfers from low to high Z species, whereas the

magnetic moment transfer is much more complicated, especially when the nonmagnetic Cu substrate is involved. It is found that there exists a Slater–Pauling curve for the averaged magnetic moment, whereas no such curve exists for the MCA energy in these monolayer systems. The nonmagnetic Cu substrate systematically suppresses the averaged magnetic moments of the alloy monolayers. Meanwhile it also leads the MCA energies of the alloying monolayer systems toward more positive. The spin-reorientation transition is found in both the free-standing and the Cu supported Fe–Co and Fe–Ni monolayers with the transition at lower Fe concentrations in the supported case. Although the simple rigid-band filling model successfully explains the averaged magnetic moment, it is, however, not adequate for describing the much more involved MCA energy of alloying monolayer systems.

Acknowledgments

This work was supported by the National Science Council of Taiwan (NSC91-2119-M-007-004). The authors thank M.T. Lin for stimulating discussions. D.S. Wang acknowledges the hospitality given by the National Center for Theoretical Sciences, Hsinchu, Taiwan, during his visit from August 2002 to February 2003, which made this collaborative work successful.

References

- [1] J.H. van Vleck, Phys. Rev. 52 (1937) 1178.
- [2] M. Kowalewski, C.M. Schneider, B. Heinrich, Phys. Rev. B 47 (1993) 8748.
- [3] A. Dittschar, M. Zharnikov, W. Kuch, M.T. Lin, C.M. Schneider, J. Kirschner, Phys. Rev. B 57 (1998) R3209.
- [4] M.T. Lin, W.C. Lin, C.C. Kuo, C.L. Chiu, Phys. Rev. B 62 (2000) 14268.
- [5] R. Thamankar, A. Ostrokhova, F.O. Schumann, Phys. Rev. B 66 (2002) 134414.
- [6] M. Dumm, B. Uhl, M. Zöfl, W. Kipferl, G. Bayreuther, J. Appl. Phys. 91 (2002) 8763.
- [7] Y. Zhao, J. Ye, C.L. Gao, B. Ma, Q.Y. Jin, J. Appl. Phys. 94 (2003) 5100.
- [8] J.G. Gay, R. Richter, Phys. Rev. Lett. 56 (1986) 2728.
- [9] J.G. Gay, R. Richter, J. Appl. Phys. 61 (1987) 3362.
- [10] D.S. Wang, R.Q. Wu, A.J. Freeman, Phys. Rev. Lett. 70 (1993) 869.
- [11] D.S. Wang, R.Q. Wu, A.J. Freeman, Phys. Rev. B 48 (1993) 15886.
- [12] M. Kim, L. Zhong, A.J. Freeman, Phys. Rev. B 57 (1998) 5271.
- [13] A.B. Shick, Y.N. Gornostyrev, A.J. Freeman, Phys. Rev. B 60 (1999) 3029.
- [14] J. Hong, R.Q. Wu, Phys. Rev. B 67 (2003) 20406.
- [15] G.H.O. Daalderop, P.J. Kelly, M.F.H. Schuurmans, Phys. Rev. B 50 (1994) 9989.
- [16] B. Újfalussy, L. Szunyogh, P. Bruno, P. Weinberger, Phys. Rev. Lett. 77 (1996) 1805.
- [17] G.Y. Guo, D.J. Roberts, G.A. Gehring, Phys. Rev. B 59 (1999) 14466.
- [18] X. Qian, W. Hübner, Phys. Rev. B 64 (2001) 92402.
- [19] W. Guo, D.L. Lin, Phys. Rev. B 67 (2003) 224402.
- [20] G. Kresse, J. Hafner, Phys. Rev. B 48 (1993) 13115; G. Kresse, J. Furthmüller, Comput. Mater. Sci. 6 (1996) 15; G. Kresse, J. Furthmüller, Phys. Rev. B 54 (1996) 11169.

- [21] P.E. Blöchl, Phys. Rev. B 50 (1994) 17953;
G. Kresse, J. Joubert, Phys. Rev. B 59 (1999) 1758.
- [22] J.P. Perdew, Y. Wang, Phys. Rev. B 45 (1992) 13244.
- [23] G.A. Somorjai, Chemistry in Two Dimension Surface, Cornell University Press, Ithaca, 1981.
- [24] D.S. Wang, R.Q. Wu, A.J. Freeman, J. Appl. Phys. 73 (1993) 6745.
- [25] R.Q. Wu, L. Chen, A.J. Freeman, J. Appl. Phys. 81 (1997) 4417.
- [26] G.H. Aylward, T.J.V. Findlay, SI Chemical Data, fourth ed., Wiley, New York, 1982.
- [27] A.J. Freeman, R.Q. Wu, J. Magn. Magn. Mater. 100 (1991) 497.
- [28] D.S. Wang, R.Q. Wu, A.J. Freeman, J. Magn. Magn. Mater. 129 (1994) 237.